Is Multicell Interference Coordination Worthwhile in Indoor Wireless Broadband Systems?

Du Ho Kang, Ki Won Sung, and Jens Zander
KTH Royal Institute of Technology, Wireless@KTH, Stockholm, Sweden
Email: {dhkang, sungkw, jenz}@kth.se

***Abstract*—The rapid growth in demand for mobile and nomadic wireless access forces the use of more and more base stations (BSs). In such dense networks, various techniques for multicell interference coordination have been investigated. However, whether or not the interference coordination provides cost benefit compared with a loosely coordinated system is not obvious because the tight coordination at PHY-layer is likely to need an expensive high-speed backbone infrastructure. In this paper, we assess the worthiness of the tight interference coordination, referred to as coordination gain, in various indoor environments. We compare a hypothetical interference-free system as an upper bound with a simple interference-limited system opportunistically avoiding interference. The range of possible coordination gain is examined for various wall losses, path loss exponents, building shapes, and deployment density. Results show that substantial gain can be achieved in dense deployment at open areas with low path loss exponent, e.g., lightly furnished offices partitioned with soft walls. Nevertheless, the coordination gain significantly drops in the presence of marginal wall loss regardless of the other environmental factors.**

I. Introduction

As a mobile broadband access widely spreads out, a recent survey reports that the orders of magnitude of more mobile data traffic will be generated at indoors in the near future [1]. Obviously, operators will seek a low-cost and high data rate indoor system to meet the unrelenting capacity demand. Inter-cell interference is one of the limiting factors for a downlink transmission in multicell environments. For enhancing the system capacity, various multicell interference coordination schemes were proposed [2]. Several studies investigated the system capacity in the ideal case where all base stations (BSs) know global knowledge by instantaneously exchanging information via the backhaul with unlimited capacity [3]–[6]. The authors of [7], [8] also considered a more realistic finite backhaul capacity for interference coordination. However, such tightly coordinated system needs dedicated backhaul installation to share channel state information (CSI) or user data streams among BSs in order to mitigate or cancel inter-cell interference.

Alternatively, the extent of interference coordination can be lowered by means of fully distributed operations or limited information sharing via existing IP connections [9]. A probabilistic approach has been adopted in the widely deployed Wi-Fi systems, i.e., distributed coordination function (DCF). A number of different distributed schemes have also been proposed in cellular systems [10]–[16]. The authors of [10]–[12] proposed distributed iterative algorithms based on broadcast message in the air, e.g., the gradient of interference when channel state varies slowly enough until the algorithm converges. In [13], [14], the random shuffling of resource blocks for transmission was considered to opportunistically avoid co-channel interference. Beside, [15], [16] proposed algorithms to exploit the statistical information, e.g., the average number of users per cell, which can be exchanged via low-cost backhaul.

Although the tighter interference coordination with more knowledge certainly provides better system capacity [9], this comes along with extra infrastructure cost in the deployment perspective, e.g., dedicated optical fibers to instantaneously share information among BSs [6]. Accordingly, it is crucial to know if such tight interference coordination is worthwhile compared with the loosely coordinated system. Moreover, due to the wide variety of in-building structures that leads to different interference characteristics [17], the tightly coordinated system may lose its performance advantage in some environments. Overall, the benefit of interference coordination has not been explicitly assessed yet despite the importance of quantitative analysis in the multitude of indoor environments.

In this paper, we aim to explore the worthiness of coordination by explicitly quantifying the performance gain of multicell interference coordination with different environmental factors, which have been largely ignored in the literature. We aim to address the following questions:

- How much interference coordination gain can be potentially achieved?
- In which type of indoor environments is the coordination worthwhile?

For this, we compare a hypothetical interference-free system and a loosely coordinated system which employs probabilistic interference mitigation. Two simplified building structures are considered where we assess the coordination gain depending on wall loss, path loss exponent, and deployment density. The remainder of the paper is organized as follows: we describe the general network model and indoor environments in Section II. In Section III, we discuss two inter-cell interference coordination models. Section IV provides numerical results, and then we draw a conclusion in Section V.

II. System Model

A. Radio Network Model

For simplicity of the exposition, we investigate two indoor building shapes as depicted in Fig. 1 where internal walls

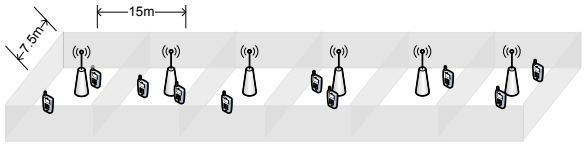

(a) Corridor building shape ($N_{BS} = 6$)

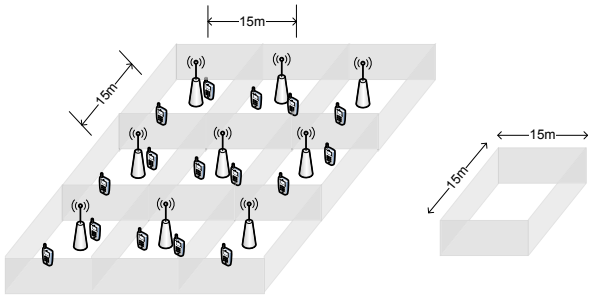

(b) Square building shape ($N_{BS} = 3 \times 3$)

Fig. 1. Indoor models and BS deployment examples

evenly divide a finite service area to create the equal size of 15 m $\times$ 15 m partitions. Note that real indoor environments may be irregular, e.g., uneven partition size and asymmetric building shapes. More various indoor environment scenarios can be explored as a future work. Then, we assume that N_{BS} single-antenna BSs are deployed in both building shapes on the same frequency band. As illustrated in Fig. 1(a)–(b), BSs are placed such that the same per-BS coverage is maintained. Although this may not be the optimal deployment due to boundary effects in the finite service area, it can reflect one of realistic indoor deployment cases which follow a basic planning guideline given in a technical manual [18]. In the above premise, let us focus the downlink transmission. Then, users experience distinct inter-cell interference characteristic depending on the building shape. A user at the corridor shape in Fig. 1(a) can be surrounded by the fewer number of neighboring interferers than one at the square shape in Fig. 1(b) where interferers exist on the vertical side as well.

It is also assumed that single user with single-antenna is uniformly distributed in a given cell at a given time. Note that the cell covered by a BS is defined as the service area in which the BS provides the highest average received signal strength to a user. This represents a fully loaded system and equal time-sharing scheduling among users in a given cell when a number of users arrive. The full load assumption may result in the optimistic gain of interference coordination since it creates the maximal interference to neighboring cells on average. However, this can provide us with a good reference scenario for upper bound analysis.

B. Propagation Model

Each radio link is affected by the path loss attenuation and Rayleigh fading. For the path loss between BS i and user j, we adopt a general Indoor Multiwall and Floor model which considers all walls intersecting the direct ray between a BS and a user [17], [19]. By assuming single floor, the path loss between BS i and user j can be dependent on the internal wall and distance as given in

$$L_{ij}^{(\mathrm{dB})} = L_0 + 10\alpha log_{10}(d_{ij}) + kL_w \ (\mathrm{dB}), \tag{1}$$

where L_0, α, d_{ij}, and k represent the constant loss, the pathloss exponent, the distance in meter between BS i and user j, and the number of walls across a BS i and a user j, respectively. Note that L_w is the constant loss per wall since we assume the homogenous indoor materials for the analysis simplicity. Also, α depends on the size or the surroundings of the partitions as well as operating frequency. In general, the bigger size of partitions with hard obstacles at higher frequency creates the higher α [17], [20], [21].

Additionally, we assume a small-scale Rayleigh fading channel component z_{ij} which is characterized by independent zero-mean unit-variance complex Gaussian distribution. By assuming rich scattering, all channels are perfectly uncorrelated. This can be justified by a fact that BSs and users are sufficiently separated. Then, let us define the complex channel response between BS i and user j as

$$h_{ij} = \sqrt{L_{ij}} z_{ij}. \tag{2}$$

Note that L_{ij} represents the linearly scaled path gain, i.e., $L_{ij} = 10^{\frac{-L_{ij}^{(\mathrm{dB})}}{10}}$. Then, a complex channel coefficient matrix is denoted by $\mathbf{H} = \{\mathrm{h_{ij}}\}$. Due to independent channel fading and user placement, $\mathbf{H}$ becomes a N_{BS} by N_{BS} square matrix with the full rank. Also, the channel gain g_{ij} can be computed from squaring the amplitude of h_{ij}, i.e., $g_{ij} = |h_{ij}|^2$.

III. Inter-cell Interference Coordination

In order to quantify the coordination gain in the downlink transmission, we consider two interference coordination systems as an upper bound and a lower bound, respectively: 1) a hypothetically interference-free system where both BSs and users fully cooperate and know ideal knowledge, and 2) a loosely coordinated system which probabilistically mitigates inter-cell interference.

A. Hypothetical Coordination with Ideal Knowledge

The aim of this subsection is to explore the maximum achievable performance of intercell interference coordination for the network configurations described in the previous section. In this regard, we employ several assumptions which are ideal and somewhat impractical to fulfill in real environments.

First, we assume that users report the perfect CSI of both signal and interfering links to their serving BSs via ideal feedback channels and BSs share them for joint processing. The availability of CSI allows BSs to coordinate their signaling strategies, e.g., power allocation and beamforming directions [22]. Second, the BSs are connected by high-capacity delay-free backhaul so that they can share the data stream of their respective users as well as the CSI information [6]. Then, a tight interference coordination can be achieved such that all BSs jointly transmit designed waveforms to the users. In this

case, the concept of an individual serving BS for one user disappears since multiple antennas belonging to different BSs can be simultaneously utilized to send data streams to a user. Besides the ideal knowledge at the BSs, we further assume that users fully cooperate to share CSIs and received signals.

In principle, such a full cooperation transforms the multicell network into a N_{BS} by N_{BS} virtual MIMO channel. In practical systems, full cooperation and ideal knowledge by users may not be realized due to considerable signaling overhead. Also, BSs can be linked by limited-capacity backhaul. However, the hypothetical system provides the upper bound of system performance below which the performance of any practical systems stays. The practical constraints on users and backhaul capacity need to be further investigated as a future work.

In this hypothetical system, it is well known that the optimal solution to maximize aggregate data rates is water-filling power allocation at transmitters, i.e., BSs for our case, with appropriate joint precoding and decoding [23], [24]. To obtain the optimal precoding and decoding vectors, we can simply apply singular value decomposition (SVD) in $\mathbf{H}$ matrix. The precoding and decoding vectors make $\mathbf{H}$ diagonalized by creating N_{BS} interference-free channels. Then, we can compute the optimal data rate in the interference-free link for a user j as follows:

$$R_j^{ideal} = \log_2\left(1 + \text{SNR}_j\right) \text{ (bps/Hz)}, \tag{3}$$

where

$$\text{SNR}_j = \frac{\lambda_j^2 P_j^*}{N_0}. \tag{4}$$

Here, λ_j is the channel eigenvalue corresponding to user j of H. Note that P_j^* can be obtained from water-filling power allocation on the channel eigenvalue [23]:

$$P_j^* = \left(\mu - \left(\frac{\lambda_j^2}{N_0}\right)^{-1}\right)^+, \tag{5}$$

where μ is chosen such that $\sum_j P_j^* = P_{tot}$. Note that $(\cdot)^+$ is zero if its argument is negative. We here presume the sum power constraint which reflects the power pooling among BSs. For the comparison with a lower bound, let us restrict ourselves to $P_{tot} = N_{BS}P_t$ where P_t denotes constant individual BS transmit power in the loosely coordinated system in the following subsection. Therefore, the system capacity of the hypothetical system is given by

$$C_{ideal} = E\left[\sum_{j\in \text{U}} R_j^{ideal}\right], \tag{6}$$

where the user set served by the BSs at a given time is denoted by U.

B. p-persistent Opportunistic Transmission

The forementioned hypothetical system needs, besides the other challenging requirements, costly dedicated backhaul on which information can be instantaneously shared among BSs. An option to lower the dedicated backhaul cost is to use IP-based broadband connections already built in the buildings. Generally, these broadband connections are provided in a best-effort basis. Thus, it is difficult to share instantaneous channel matrix or user data stream in a guaranteed manner. It will be only the long-term local information, e.g., user distribution or load statistics per cell, that can be consistently shared among BSs to aid the statistical multicell interference coordination.

As the representative of a loosely coordinated system, we consider a statistical information based interference coordination which we compare with the hypothetical MIMO system. Specifically, we adopt probabilistic multicell interference mitigation where BSs opportunistically avoid concurrent transmissions in fully shared frequency band [11], [13], [14]. In this scheme, each BS is randomly activated by following an activation probability p which can be initially configured in the deployment phase or be automatically adapted according to environmental changes, e.g., the change of BS topology or the statistics of user distribution. It is worth to noting that p is chosen once at the deployment phase since we restrict our attention to a stationary system in a sense that user statistics and BS topology remain same. At a given time, the data rate of a user j served by its activated BS i can be computed by

$$R_j = \log_2\left(1 + \text{SINR}_j\right) \text{ (bps/Hz)}, \tag{7}$$

where

$$\text{SINR}_j = \frac{g_{ij}P_t}{I_j + N_0}. \tag{8}$$

Note that I_j represents aggregate interference received at a serving user j from all active neighboring BSs which transmit with fixed power P_t at a given time. Then, let us define the system capacity for a given p probability as

$$C_{prob}(p) = E\left[\sum_{j\in \text{U}^p} R_j\right] \text{ (bps/Hz)}. \tag{9}$$

We here use a term U^p for the user set served by activated BSs at a given time.

While leaving the practical method of configuring p out of scope in this paper, we assume that all BSs are always assigned with the optimal p^* to provide the best performance in a given indoor environment. For any indoor environments, p^* can be obtained by solving the following optimization problem:

$$\begin{aligned} \text{maximize} \quad & C_{prob}(p) \\ \text{subject to} \quad & \nu_{prob}(p) < \beta \\ & \theta_{min} \le p \le \theta_{max} \end{aligned}$$

where $\nu_{prob}(p) = \Pr(\text{SINR}_j < \gamma_t)$ represents the outage probability of serving users from the activated BSs with minimum SINR threshold γ_t. Note that θ_{min}, θ_{max}, and β represent the minimum activation probability, the maximum activation probability, and outage probability threshold, respectively. In order to obtain $C_{prob}(p^*)$, we employ the fine-grained quantization of p, and perform an exhaustive search to find the best estimated $C_{prob}(p)$ subject to $\nu_{prob}(p) < \beta$.

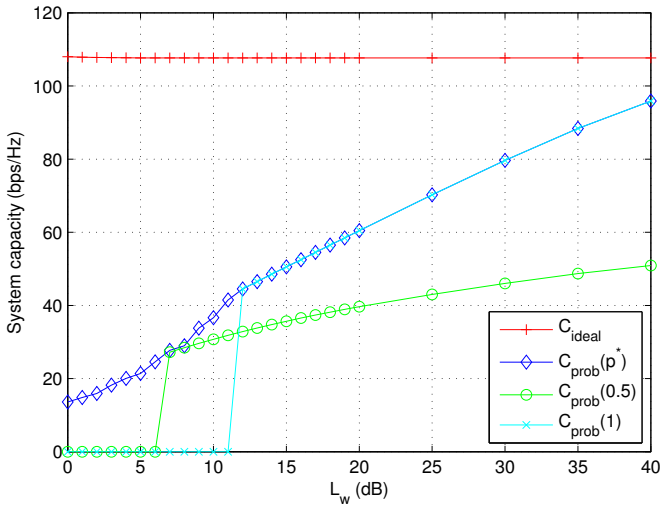

Fig. 2. System capacity according to L_w (Corridor shape with $N_{BS} = 6$ and $\alpha = 3$).

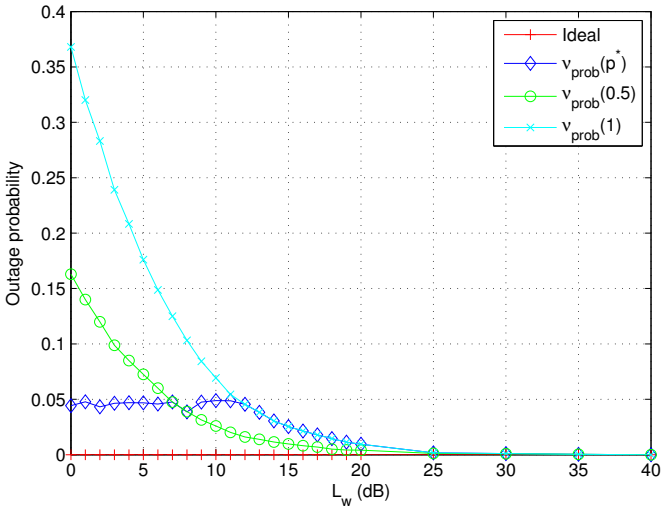

Fig. 3. Outage probability according to L_w (Corridor shape with $N_{BS} = 6$ and $\alpha = 3$).

C. Coordination Gain

By comparing $C_{prob}(p^*)$ with C_{ideal} of the hypothetical system where ideal MIMO channel capacity can be achieved, we can quantify *coordination gain* defined as

$$Coordination\ gain := \frac{C_{ideal}}{C_{prob}(p^*)}.$$

This reflects the average system performance improvement over the statistical information based coordination by instantaneously coordinating the inter-cell interference. Higher coordination gain can be interpreted as the larger cost benefit of interference coordination for a given extra infrastructure cost.

TABLE I
AVERAGE WALL LOSS ACCORDING TO COMMON BUILDING MATERIAL [17]

Material Type	Loss (dB)	Center Frequency (MHz)
All metal	26	815
Concrete block wall	13-20	1300
Empty cardboard	3-6	1300
Light textile	3-5	1300

IV. Numerical Results

A. Simulation Parameters

In the numerical evaluation, $L_0 = 37$ dB, $N_0 = -95$ dBm, and $P_t = 20$ dBm are used, respectively. We also limit our evaluation with $\gamma_t = 6$ dB and $\beta = 0.05$. For a given L_w, we average the performance over 1000 different channel realizations to estimate C_{ideal} and $C_{prob}(p^*)$.

B. Wall Effects on Coordination Gain

Fig. 2 and 3 illustrate the system capacity and the outage probability of two systems in the corridor shape when $N_{BS} = 6$. Since each BS is located at the center of each partition, all users in each partition are likely connected to the BS in the same partition. As a result, C_{ideal} is constant with almost zero outage probability regardless of L_w since the desired signals are not weakened by the walls while the interference is perfectly eliminated. Note that the outage in the hypothetical interference-free system can occur when the optimal waterfilling assigns insufficient power on a particular link to maximize the sum of rates at a given time. However, as shown in 3, it rarely happens in the considered evaluation scenario so that the hypothetical system easily meets the same outage probability constraint $\beta = 0.05$ imposed in the p-persistent coordination. On the other hand, the p-persistent coordination is heavily affected by L_w due to inter-cell interference. With the fixed p allocation, it may violate outage constraint β in relatively small L_w due to excessive interference from neighboring BSs. By lowering p, the system can satisfy the outage constraint thanks to the conservative transmission, but it has fewer opportunity to transmit, i.e., lower system capacity. With the optimal p^* configuration, $C_{prob}(p^*)$ increases as L_w grows while meeting the outage constraint.

Fig. 4(a)–(b) illustrates the effects of different α and building shapes on the coordination gain, respectively. Lower α generates more interference since interference can reach further users. Besides, the corridor shape has less coordination gain than the square shape since users in the corridor hurts only from horizontally deployed BSs due to the building structure. Thus, the figures show that the square shape and the smaller α have higher coordination gain since they create larger interference which can be totally removed in the hypothetical system. Nevertheless, the gain significantly drops as L_w increases regardless of the building shape and α. For instance, Fig. 4(a) shows that the gain in the corridor shape drops by 63% with $L_w = 10$ dB regardless of α. Also, in Fig. 4(b), the gain decreases by 63% and 70% with $L_w = 10$ dB in the corridor and the square shape, respectively. In Table I, several

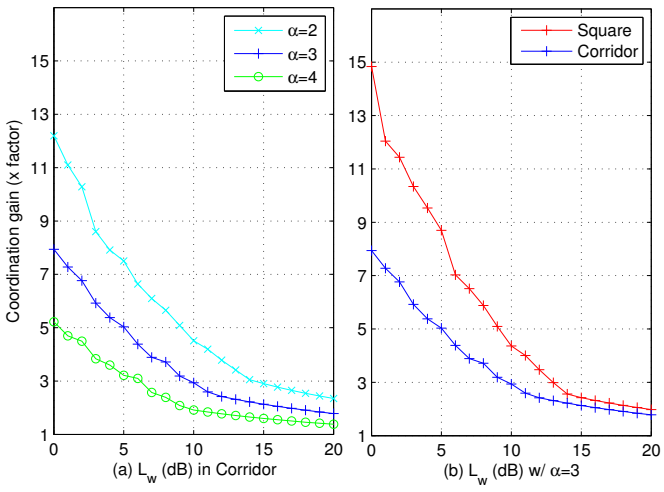

Fig. 4. Coordination gain according to wall loss ($N_{BS} = 6$).

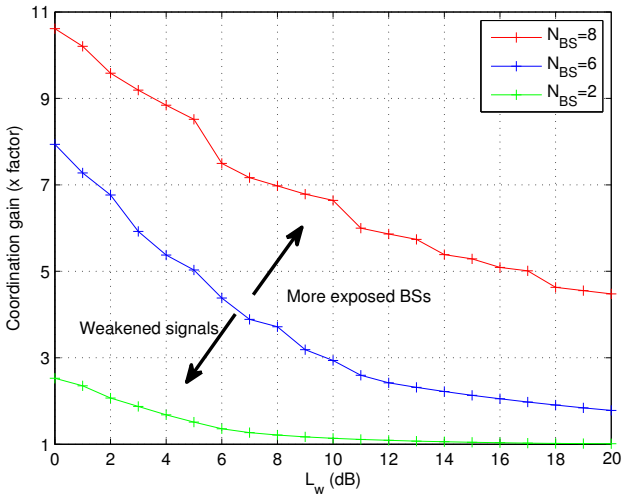

Fig. 5. Coordination gain in different deployment density (Corridor shape with $\alpha = 3$).

examples of average wall loss are listed according to the typical materials at different center frequency. It shows that 10 dB attenuation corresponds to typical concrete block walls which are usually used for dividing large areas, e.g., office divisions or households in apartments.

C. Deployment Density and Coordination Gain

Depending on the user demand, operators can deploy more (fewer) number of BSs to increase (decrease) the system capacity in a given service area. However, more BSs cause more downlink interference in general. We explore the effects of deployment density on the coordination gain. Fig. 5 provides how the coordination gain is changed with more or fewer BSs deployment in the corridor shape. Note that each BS is evenly placed in a horizontal axis to cover the same geographical area. Since there are six partitions with five walls, at least one of BSs faces with another BS without any wall separation when $N_{BS} = 8$. In the p-persistent transmission, such exposed BS loses any benefit from wall shielding so that the performance deterioration is inevitable due to the more conservative transmission setting. Consequently, the coordination gain curve is shifted toward right in the figure. On the other hand, there can be multiple walls between serving users and associated BSs when $N_{BS} = 2$. Due to the wall penetration loss in traversing signals, some of users positioned in partitions without BSs experience much weakened signals which do not occur when N_{BS} is more than the number of partitions. Accordingly, the capacity of the hypothetical system drops regardless of the interference elimination to let the coordination gain curve shifted leftward.

V. Conclusion

We investigated the potential benefit of practical multicell interference coordination. For this, we quantitatively assessed the optimistic performance gain of coordination on purpose in the various range of indoor environments. We compared a hypothetical interference-free system as the upper bound and a loosely coordinated system with probabilistic interference mitigation as the lower bound. The coordination gain was evaluated under various wall loss, path loss exponents, building shapes, and deployment density.

Numerical results demonstrate that the multicell interference coordination is not always worthwhile. In open areas such as conference halls, the coordination can ideally provide the substantial gain especially when BSs are densely deployed. However, the gain considerably declines with marginal increase in wall loss between BSs regardless of other environmental factors, e.g., 60–70% drop in the presence of 10 dB wall loss which corresponds to the typical brick wall in offices. This suggests that the cost of dedicated backhaul to enable the tight coordination may not be compensated in network deployments with reasonable wall losses. As a future work, the refined coordination gain should be evaluated especially where significant gain is identified by comparing a more practical upper bound with a lower bound in a more realistic load and shared backhaul scenarios.

References

[1] "Traffic and market data report," *White Paper, Ericsson*, Nov. 2011.
[2] K. Karakayali, G. J. Foschini, and R. A. Valenzuela, "Network coordination for spectrally efficient communications in cellular systems," *IEEE Wireless Communications Magazine*, pp. 56–61, 2006.
[3] S. Shamai and B. Zaidel, "Enhancing the cellular downlink capacity via co-processing at the transmitting end," in *Proc. IEEE VTC*, Rhodes, Greece, May 2001.
[4] W. Yu and T. Lan, "Transmitter optimization for the multi-antenna downlink with per-antenna power constraints," *IEEE Transactions on Signal Processing*, vol. 55, no. 6, pp. 2646–2660, Jun. 2007.
[5] S. Jing, D. Tse, J. B. Soriaga, J. Hou, J. E. Smee, and R. Padovani, "Multicell downlink capacity with coordinated processing," *EURASIP Journal Wireless Commun. Networking*, 2008.
[6] D. Gesbert, S. Hanly, H. Huang, S. S. Shitz, O. Simeone, and W. Yu, "Multicell MIMO cooperative networks: A new look at interference," *IEEE Journal on Selected Areas in Communications*, vol. 28, no. 9, pp. 1380–1408, Dec. 2010.
[7] O. Simeone, O. Somekh, H. V. Poor, and S. Shamai, "Downlink multicell processing with limited-backhaul capacity," *EURASIP Journal on Advances in Signal Processing*, vol. article ID 840814, May 2009.

[8] R. Zakhour and D. Gesbert, "Optimized data sharing in multicell MIMO with finite backhaul capacity," *IEEE Transactions on Signal Processing*, vol. 59, no. 12, pp. 6102–6111, Dec. 2011.

[9] S. Landstrm, A. Furuskr, K. J. on, L. Falconetti, and F. Kronestedt, "Heterogeneous networks increasing cellular capacity," *Ericsson Review*, 2011.

[10] D. A. Schmidt, C. Shi, R. A. Berry, M. L. Honig, and W. Utschick, "Distributed resource allocation schemes," *IEEE Transactions on Signal Processing*, vol. 26, no. 5, pp. 53–63, Sep. 2009.

[11] M. Andrews, V. Capdevielle, A. Feki, and P. Gupta, "Autonomous spectrum sharing for mixed LTE femto and macro cells deployments," in *Proc. IEEE INFOCOM*, San Diego, USA, Mar. 2010.

[12] K. Son, S. Lee, Y. Yi, and S. Chong, "REFIM: A practical interference management in heterogeneous wireless access networks," *IEEE Journal on Selected Areas in Communications*, vol. 29, no. 6, pp. 1260–1272, Jun. 2011.

[13] R. Bosisio and U. Spagnolini, "Interference coordination vs. interference randomization in multicell 3GPP LTE system," in *Proc. IEEE WCNC*, Las Vegas, Apr. 2008.

[14] V. Chandrasekhar and J. G. Andrews, "Spectrum allocation in tiered cellular networks," *IEEE Transactions on Communications*, vol. 57, no. 10, pp. 3059–3068, Oct. 2009.

[15] I. Ashraf, H. Claussen, and L. T. Ho, "Distributed radio coverage optimization in enterprise femtocell networks," in *Proc. IEEE ICC*, Cape Town, South Africa, May 2010.

[16] J.-H. Yun and K. Shin, "Adaptive interference management of OFDMA femtocells for co-channel deployment," *IEEE Journal on Selected Areas in Communications*, vol. 29, no. 6, pp. 1225 –1241, Jun. 2011.

[17] T. S. Rappaport, *Wireless communications principles and practice*. Pearson Education, 2002.

[18] M. Unbehaun and M. Kamenetsky, "On the Deployment of Picocellular Wireless Infrastructure," *IEEE Wireless Communications Magazine*, vol. 10, no. 6, pp. 70–80, Dec. 2003.

[19] M. Lott and I. Forkel, "A multi-wall-and-floor model for indoor radio propagation," in *Proc. IEEE VTC*, New Jersey, USA, Oct. 2001.

[20] H. Hashemi, "The indoor radio propagation channel," in *Proceedings of the IEEE*, vol. 81, no. 7, Jul. 1993.

[21] M. Tolstrup, *Indoor Radio Planning, A practical guide for GSM, DCS, UMTS and HSPA*. John Wiley & Sons Ltd, 2008.

[22] B. D. Gesbert, S. G. Kiani, A. Gjendemsj, and G. E. ien, "Adaptation, coordination, and distributed resource allocation in interference-limited wireless networks," *Proceedings of the IEEE*, vol. 95, no. 12, pp. 2393–2409, 2007.

[23] E. Telatar, "Capacity of multi-antenna gaussian channels," *AT&T-Bell Labs Internal Tech. Memo.*, Jun. 1995, available: http://mars.bell-labs.com/papers/proof/proof.pdf.

[24] G. J. Foschini and M. J. Gans, "On limits of wireless communications in a fading environment when using multiple antennas," *Wireless Ppersonal Communications*, vol. 6, no. 3, pp. 311–335, Mar. 1998.